Supplementary Information

Table S1. Univariate analysis of brain metabolomics

Brain		
Metabolite	**TK2 vs WT Fold Δ**	**Pathway**
N-acetyl-l-alanine	1.8	Amino acid metabolism
N-acetyl-l-phenylalanine	1.8	
N-acetyl-l-leucine	1.7	
Norleucine	1.7	
N-acetylglycine	1.5	
4-acetamidobutanoate	1.5	
L-valine	1.5	
Ketoleucine	1.3	
5-oxo-l-proline	1.3	
Glycine	1.3	
N-acetyl-dl-serine	1.2	
L-proline	1.2	
2-hydroxyglutarate	0.9	
L-asparagine	0.9	
L-pipecolic acid	0.8	
L-tyrosine	0.8	
Alpha-aminoadipate	0.6	
Pyridoxal	1.4	Cofactor metabolism
D-pantothenic acid	1.2	
Omega-hydroxydodecanoic acid	1.7	Fatty acid metabolism
2-methylglutaric acid	1.4	
Ethylmalonic acid	1.3	
3-hydroxybutanoic acid	1.2	
Glutarate	0.9	
Glyoxylic acid	1.5	
2-amino-2-methylpropanoate	1.3	Nucleotide metabolism
Inosine 5'-phosphate	1.2	
Deoxycytidine	1.2	
Cytidine	0.8	
Guanosine	0.8	
Hypoxanthine	0.8	
2-hydroxybutyrate	1.4	Oxidative stress
Fumarate*	1.2	TCA cycle
Malate	1.1	

*Metabolites whose fold-values are differentially regulated (upregulated in TK2 vs WT in red; downregulated in blue) with significant p values <0.05. They are also shown as colored data points in Fig. S9. Blank boxes denote no significant change.

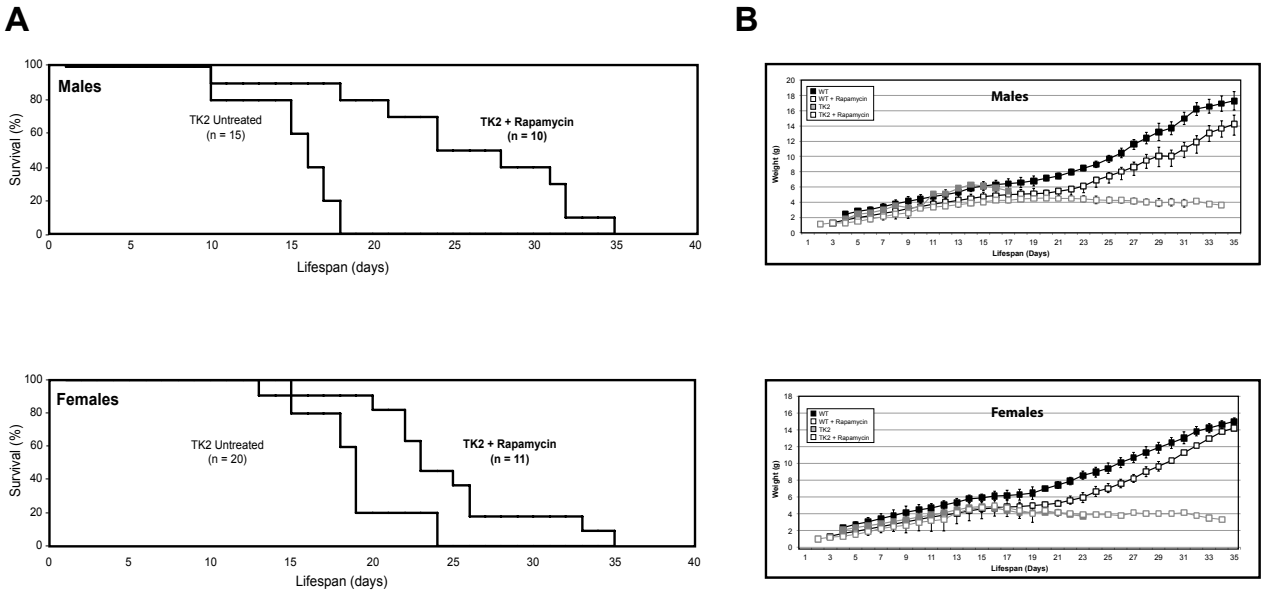

Supplementary Figure S1. Phenotypic analysis by gender. (A) Kaplan-Meyer curves. **(B)** Pup weight of rapamycin-treated and untreated litters was measured daily, and indicated for untreated WT (black filled squares), rapamycin-treated WT (black open squares), untreated TK2 (gray filled squares), and rapamycin-treated TK2 (gray open squares) mice. Error bars represent standard deviation, when applicable.

Fig. S2

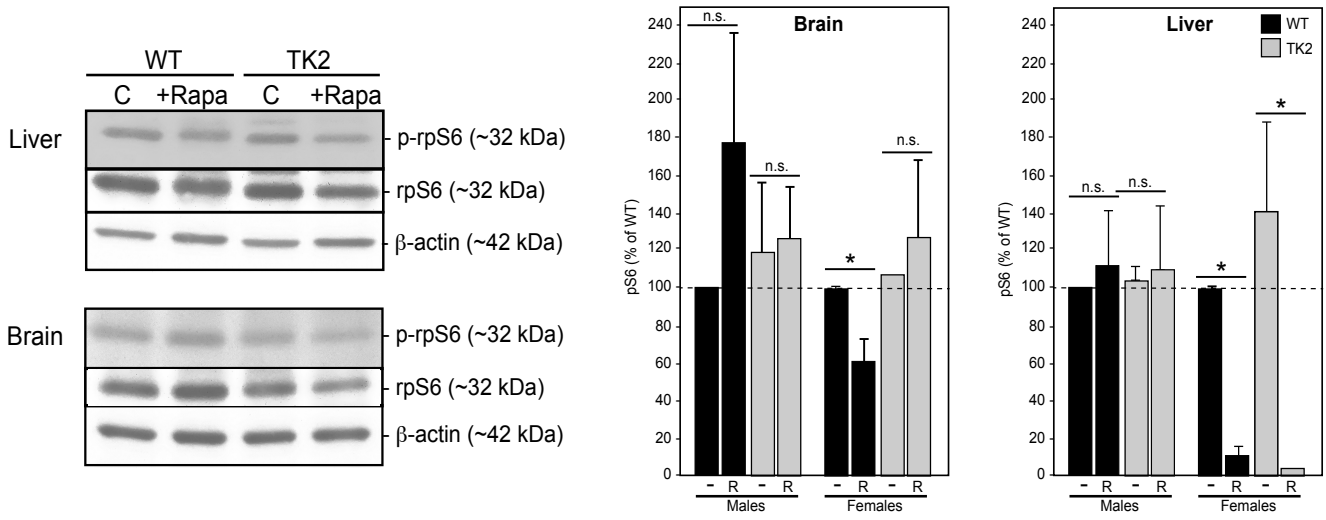

Supplementary Figure S2. Representative western blots illustrating phosphorylation of rpS6 at Ser240/244 in untreated vs rapamycin-treated WT and TK2 livers and brains from male mice, compared with total rpS6 and β-actin. Quantitation at right. Other notation as in Fig. 3.

Fig. S3

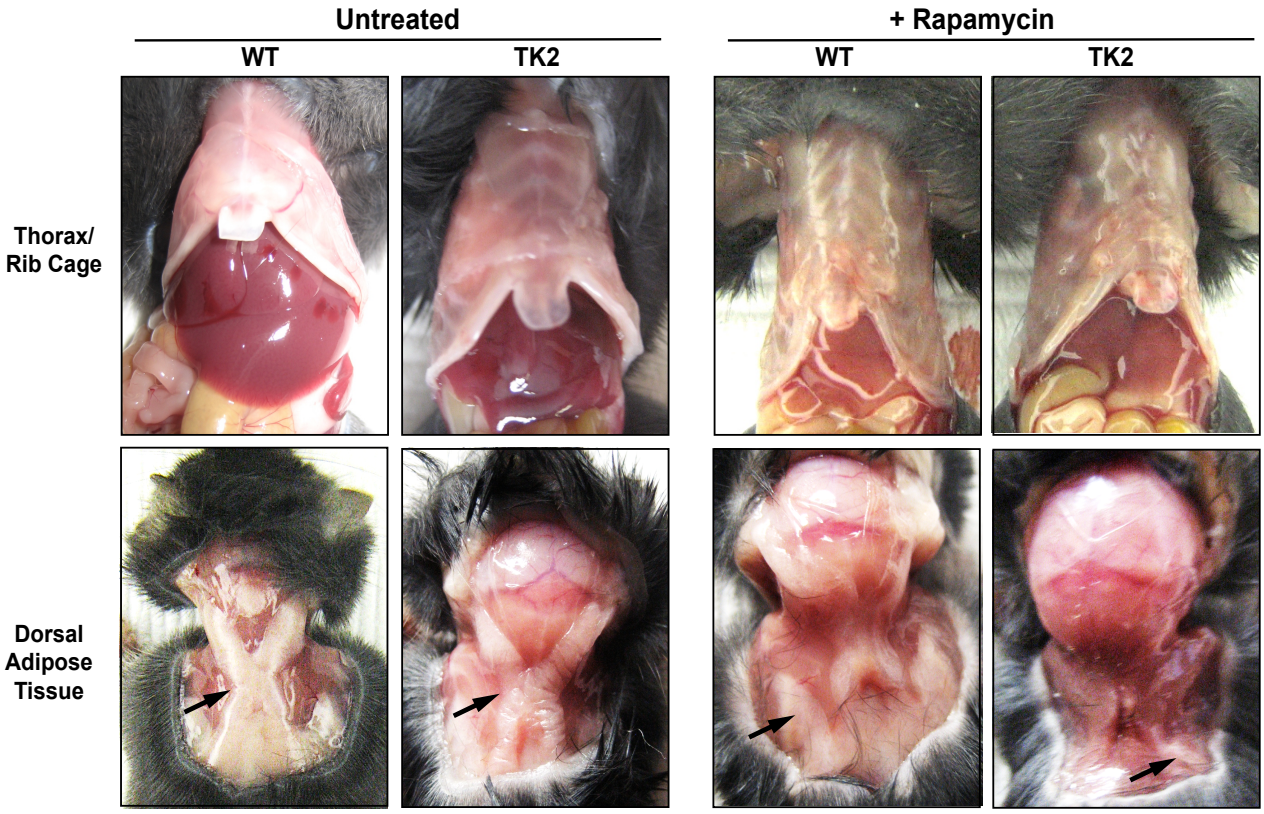

Supplementary Figure S3. Typical example of gross morphology of a "tetrad". Representative gross morphology of rapamycin-treated and untreated WT and TK2 mouse pups (16-18d). For the thorax/rib cage, note the "thinner" and more translucent appearance of the thoracic musculature in the TK2 mouse, which is accentuated by rapamycin treatment in both WT and TK2 animals. For the dorsal adipose tissue (arrows), note the loss of adiposity in the TK2 mouse, which is accentuated by rapamycin treatment in both WT and TK2 animals.

Fig. S4

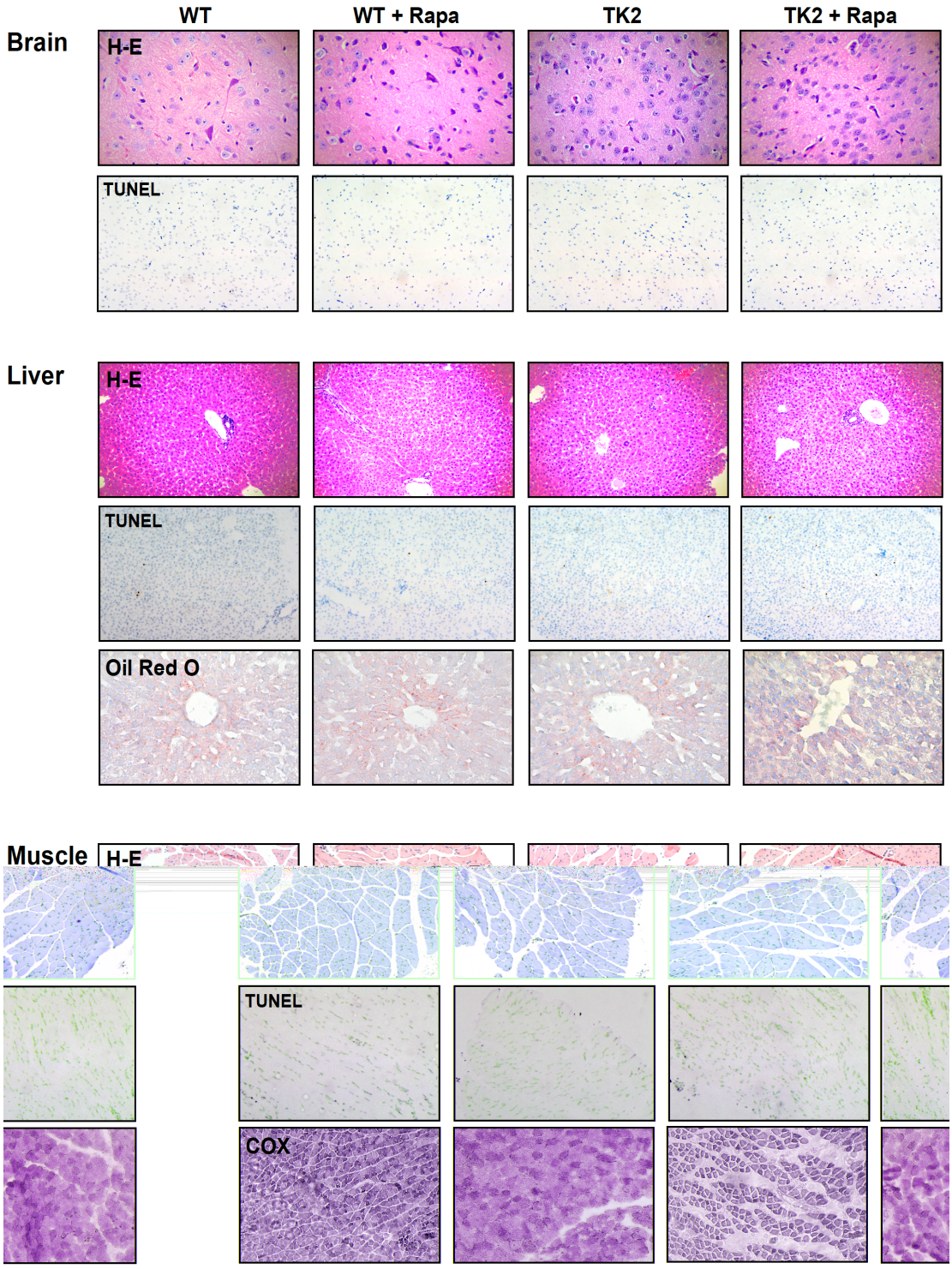

Supplementary Figure S4. Typical example of histology of a "tetrad". Representative histology of rapamycin-treated and -untreated WT and TK2 mouse pups (16-18d); brain hematoxylin & eosin (H&E) (40x) and TUNEL stain (20x), liver H&E (20x), TUNEL stain (20x), and Oil-Red-O (60x), and skeletal muscle H&E (20x), TUNEL stain (20x), and COX activity staining (20x).

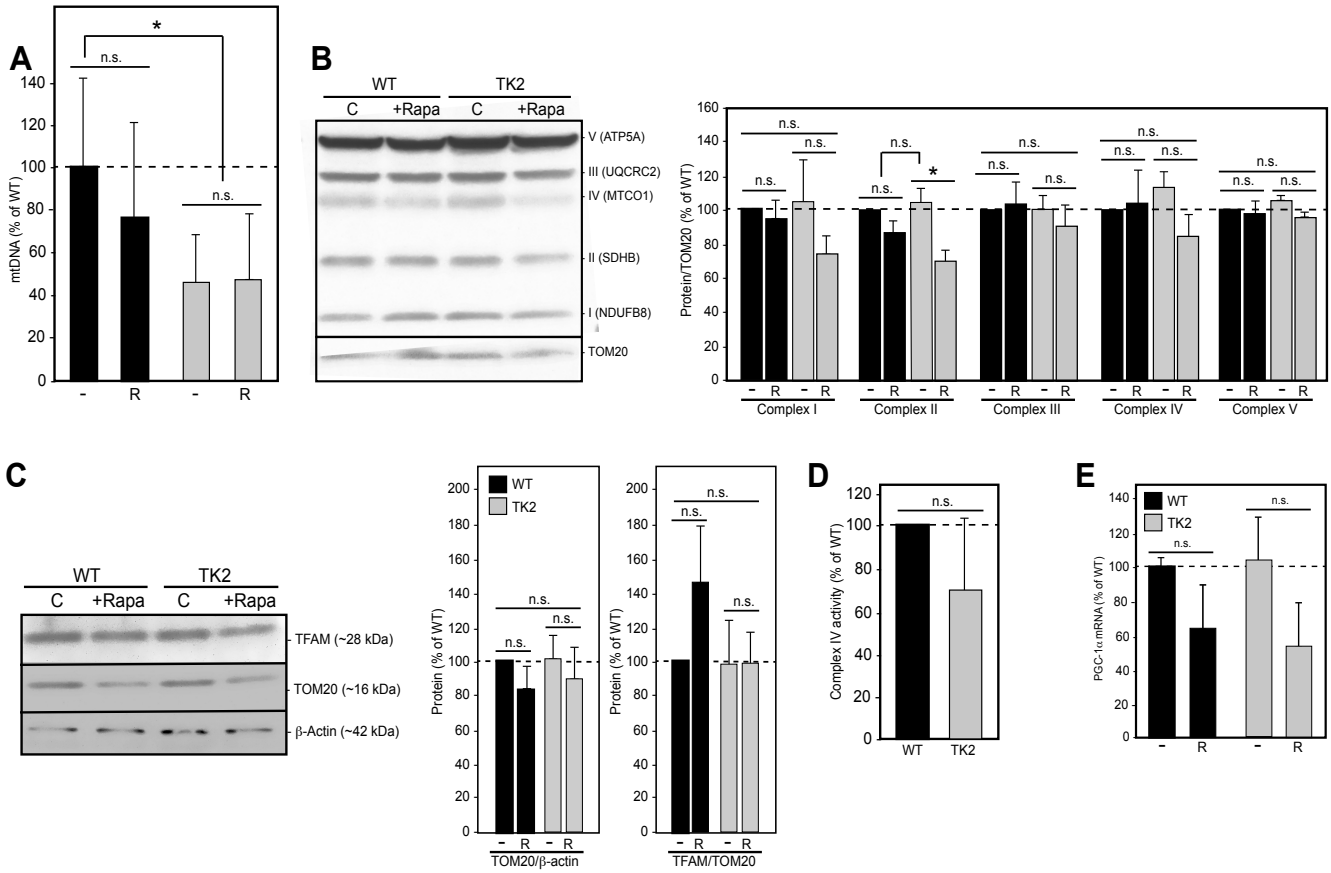

Supplementary Figure S5. Rapamycin does not affect mtDNA disease in the livers of treated TK2 mice. (A) Quantitation of liver mtDNA levels (relative to nuclear DNA [*Gapdh*]) by qPCR in 15- to 18-day-old pups (n=10, n=12, n=12, and n=10 for untreated WT, rapamycin-treated WT, untreated TK2, and rapamycin-treated TK2 mice, respectively). **(B)** Representative western blot and quantitation (n=5) of representative subunits from respiratory complexes I - V, normalized to TOM20. **(C)** Representative western blot and quantitation for TFAM (n=6), TOM20 (n=6), and β-actin (n=4); TOM20 was quantitated relative to β-actin (n=4) and TOM20 relative to TFAM (n=6). **(D)** Complex IV activity was measured in isolated mitochondria from untreated WT (n=4) and TK2 (n=5) liver using a Seahorse XFe24 flux analyzer and the standard electron flow assay; values were normalized to total mitochondrial content. **(E)** Quantitation of liver PGC-1α signal by qRT-PCR (n=5). For all graphs, values are shown as percentages relative to untreated WT, with error bars indicating standard deviation, and significance tested by Welch's t-test at 95% confidence. Other notation as in Fig. 3.

Fig. S6

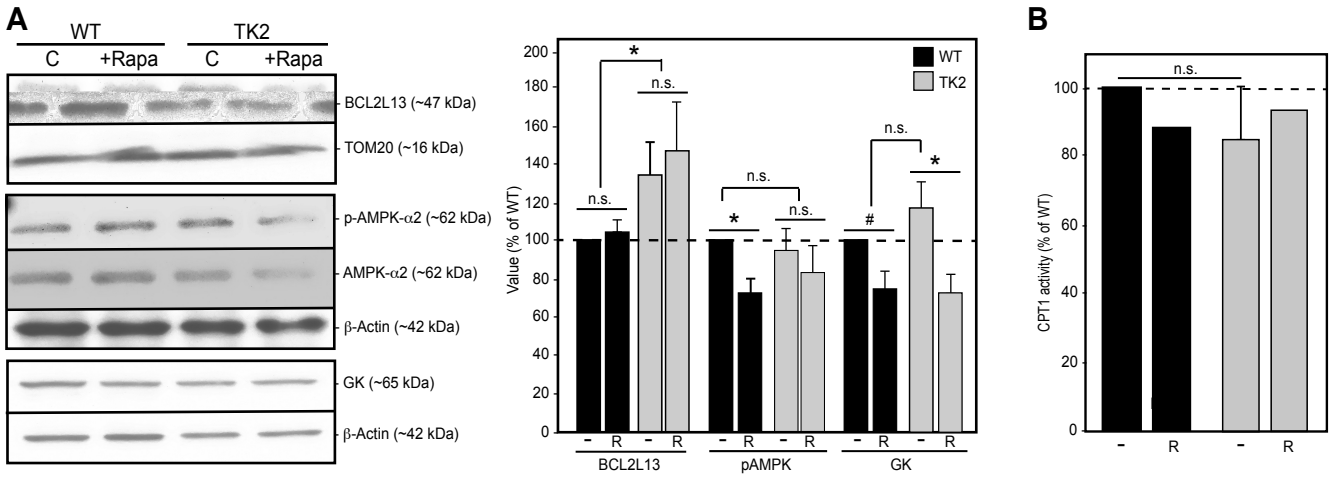

Supplementary Figure S6. Canonical pathways of rapamycin are not perturbed in TK2 livers. **(A)** Representative western blots and quantitation for BCL2L13 normalized to TOM20 (n=4), pAMPK normalized to β-actin (n=6), and glucokinase (GK) normalized to β-actin (n=4). **(B)** Assay of CPT1 activity (n=4 for treated; n=2 for untreated). For all graphs, values are shown as percentages relative to untreated WT, with error bars indicating standard error *, $p<0.05$; #, $p<0.07$. Other notation as in Fig. 3.

Fig. S7

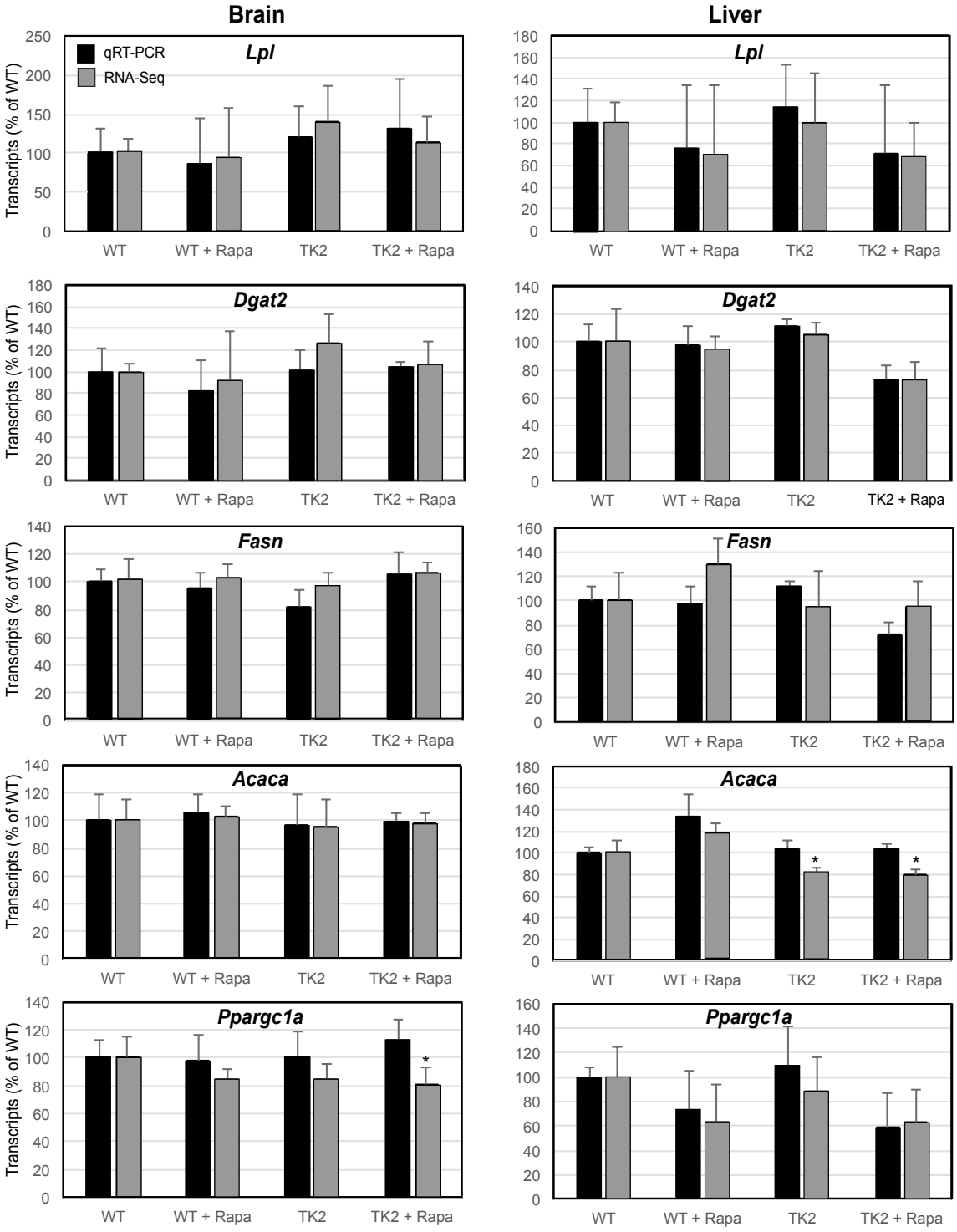

Supplementary Figure S7. Validation of RNA-Seq data. Side-by-side comparisons of transcript levels of the five indicated genes in brain and liver. All data are reported relative to the levels in untreated WT animals. *, $p<0.05$; n=3 for all analyses.

Fig. S8

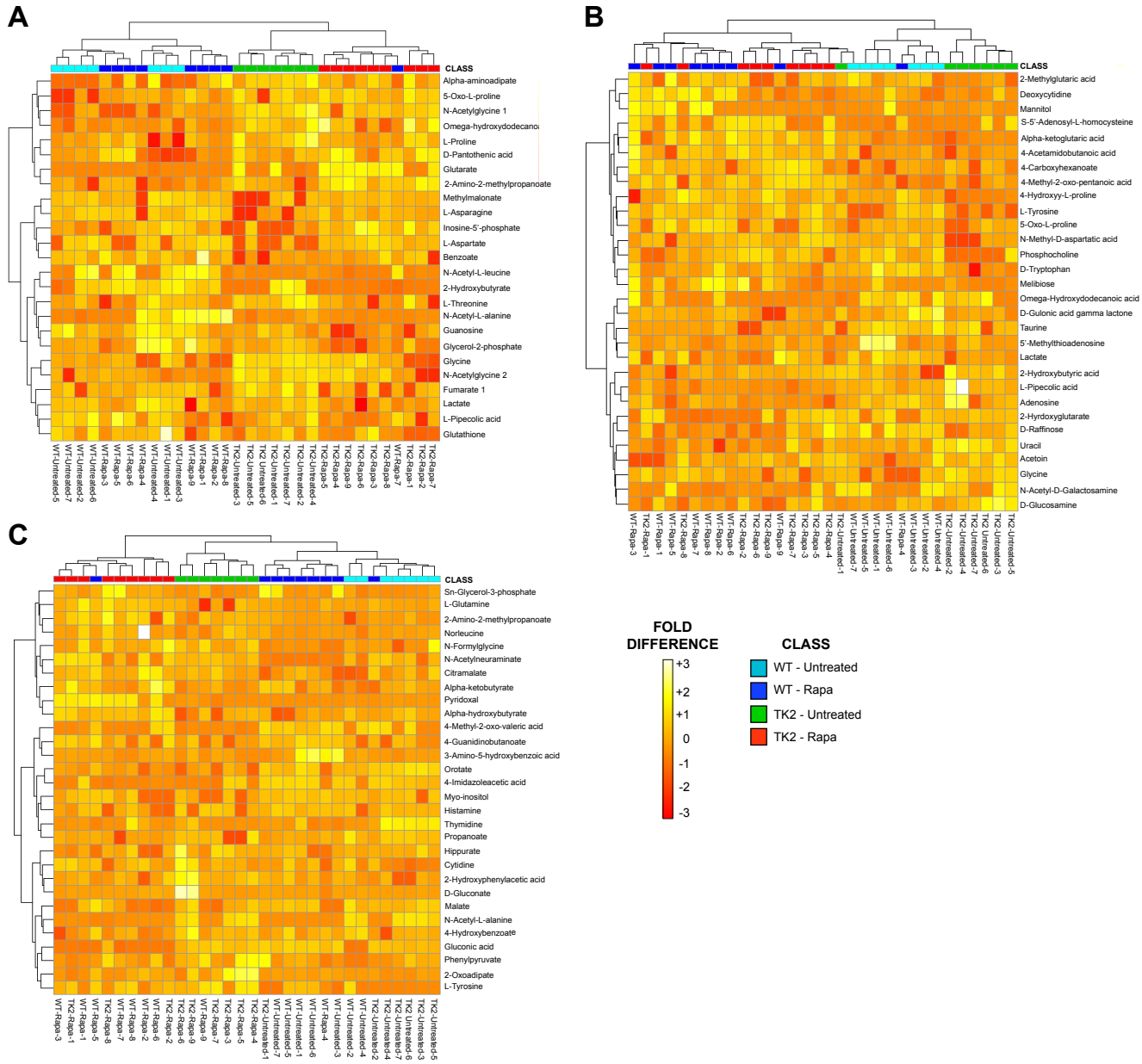

Supplementary Figure 8. Unsupervised cluster analysis of metabolomics data. Hierarchical clustering with a feature-normalized heatmap (legend shown at lower right) of all 32 mice in the 4 treatment groups, conducted using the most significantly altered metabolites, as determined by ANOVA. The top 25-30 most significant metabolites were used for brain **(A)**, and the top 30 most significant metabolites were used for liver **(B)** and plasma **(C)**.

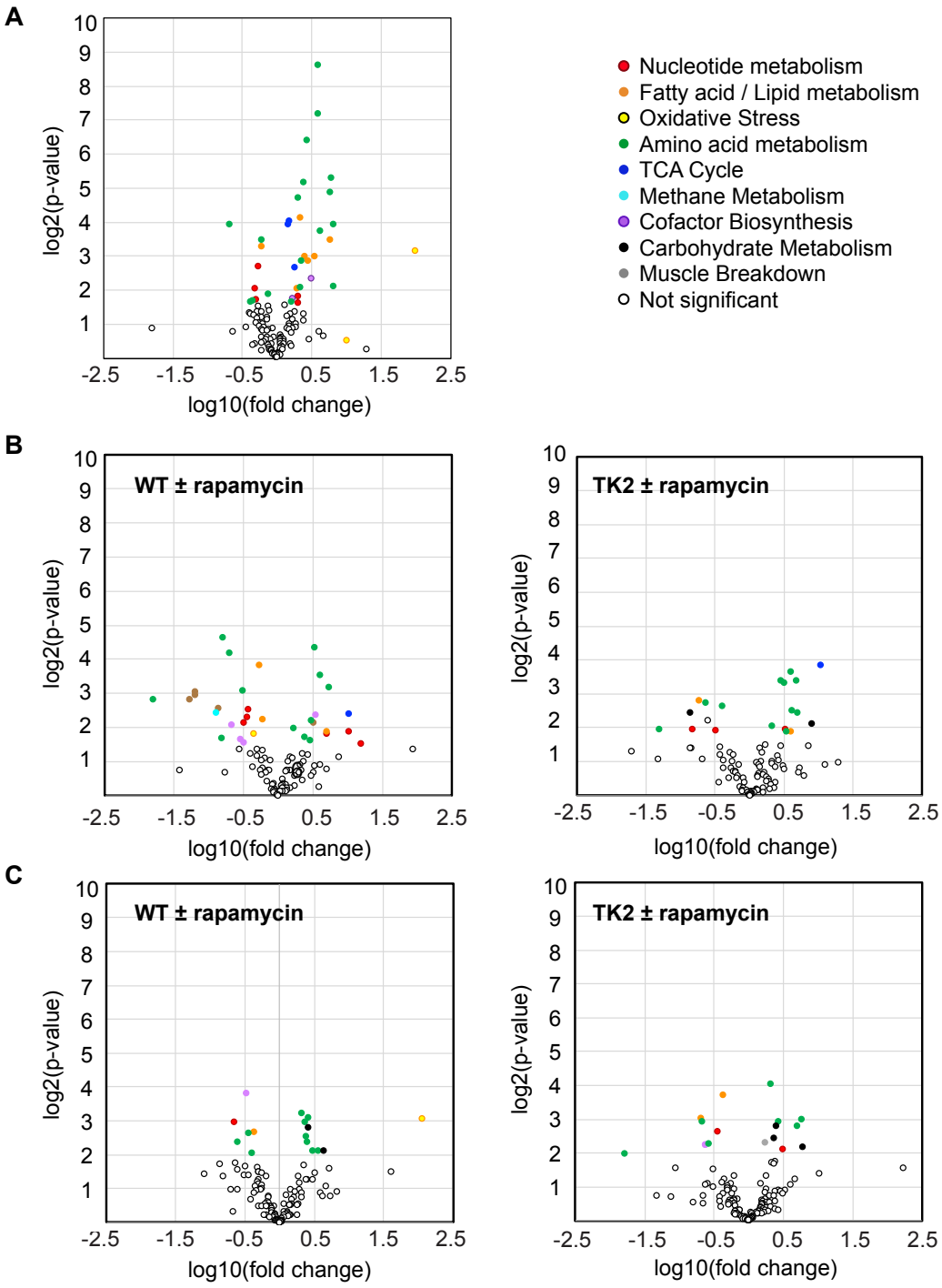

Supplementary Figure S9. Univariate analysis of metabolomics data. Univariate analysis of all identified metabolites, represented as volcano plots of log-transformed data. Colors represent pathway categorization of metabolites with significant fold-differences ($p<0.05$, FDR $q=0.1$). See also Tables 1 and S1. **(A)** Brain comparison represents fold-change in pooled TK2 vs pooled WT animals. **(B)** Liver comparison represents WT ± rapamycin (left) and TK2 ± rapamycin (right). **(C)** Plasma comparison represents WT ± rapamycin (left) and TK2 ± rapamycin (right).